Drug and light dose responses to focal photodynamic therapy of single blood vessels *in vivo*

Mamta Khurana
Eduardo H. Moriyama
Adrian Mariampillai
University of Toronto
Division of Biophysics and Bioimaging
Department of Medical Biophysics
Ontario Cancer Institute
Toronto, Ontario M5G2M9
Canada

Kimberley Samkoe
Dartmouth College
Thayer School of Engineering
8000 Cummings Hall
Hanover, New Hampshire 03755

David Cramb
University of Calgary
Department of Chemistry
Calgary, AB T2N 1N4
Canada

Brian C. Wilson
University of Toronto
Division of Biophysics and Bioimaging
Department of Medical Biophysics
Ontario Cancer Institute
Toronto, Ontario M5G2M9
Canada

Abstract. As part of an ongoing program to develop two-photon ($2\text{-}\gamma$) photodynamic therapy (PDT) for treatment of wet-form age-related macular degeneration (AMD) and other vascular pathologies, we have evaluated the reciprocity of drug-light doses in focal-PDT. We targeted individual arteries in a murine window chamber model, using primarily the clinical photosensitizer Visudyne/liposomal-verteporfin. Shortly after administration of the photosensitizer, a small region including an arteriole was selected and irradiated with varying light doses. Targeted and nearby vessels were observed for a maximum of 17 to 25 h to assess vascular shutdown, tapering, and dye leakage/occlusion. For a given end-point metric, there was reciprocity between the drug and light doses, i.e., the response correlated with the drug-light product (DLP). These results provide the first quantification of photosensitizer and light dose relationships for localized irradiation of a single blood vessel and are compared to the DLP required for vessel closure between $1\text{-}\gamma$ and $2\text{-}\gamma$ activation, between focal and broad-beam irradiation, and between verteporfin and a porphyrin dimer with high $2\text{-}\gamma$ cross section. Demonstration of reciprocity over a wide range of DLP is important for further development of focal PDT treatments, such as the targeting of feeder vessels in $2\text{-}\gamma$ PDT of AMD. © *2009 Society of Photo-Optical Instrumentation Engineers.* [DOI: 10.1117/1.3262521]

1 Introduction

The history of photodynamic therapy (PDT) dates back to the early 1900s with the observation of the effects of light and dyes on paramecia.[1,2] The current status of PDT as a treatment modality exploiting the cytotoxicity of light-activated compounds (photosensitizers) derives from the work of several pioneers, including studies by Lipson, Baldes, and Schwartz at the Mayo Clinic in the 1960s using hematoporphyrin, followed by clinical investigations by Dougherty's group at Roswell Park Cancer Institute in the 1970s.[3–5] Currently, PDT is approved in several countries for various cancers and noncancerous conditions, the latter including the wet-form of age-related macular degeneration (AMD), actinic keratosis, and localized infection, using a variety of photosensitizers and light sources.[6]

In addition to direct cell targeting with PDT, several groups have emphasized the importance of the vascular effects of this modality.[7–9] This is the basis for PDT for AMD, where the objective is to shut down the abnormal choroidal neovasculature without damaging the normal retinal blood vessels, and for other noncancerous lesions like port-wine stain. The primary pathway for the vascular effects of PDT most likely begins with initial damage to the vascular endothelial cells, leading to exposure of the vascular basement membrane and, thereby, to the creation of thrombogenic sites within the vessel lumen. This initiates a cascade of responses, including platelet aggregation, release of vasoactive molecules, leukocyte adhesion, and increases in vascular permeability and vessel constriction.[7,8] These effects have been studied in a number of model systems,[10–13] including recent work from our own group in a dorsal skin window chamber mouse model (WCM).[14]

PDT using the benzoporphyrin derivative photosensitizer verteporfin (Visudyne, QLT, Inc., British Columbia, Canada) was first approved for the treatment of wet-form AMD in 2000. This condition is a major cause of vision loss in the elderly,[15] characterized by ingrowth of new blood vessels (neovasculature) from the choriocapillaris. This leads to destruction of photoreceptors in the fovea and consequent loss

Address all correspondence to: Brian C. Wilson, University of Toronto, Division of Biophysics and Bioimaging, Department of Medical Biophysics, Ontario Cancer Institute, Toronto, Ontario M5G2M9 Canada. Tel: 416-946-2952; Fax: 416-946-6529; E-mail: wilson@uhnres.utoronto.ca
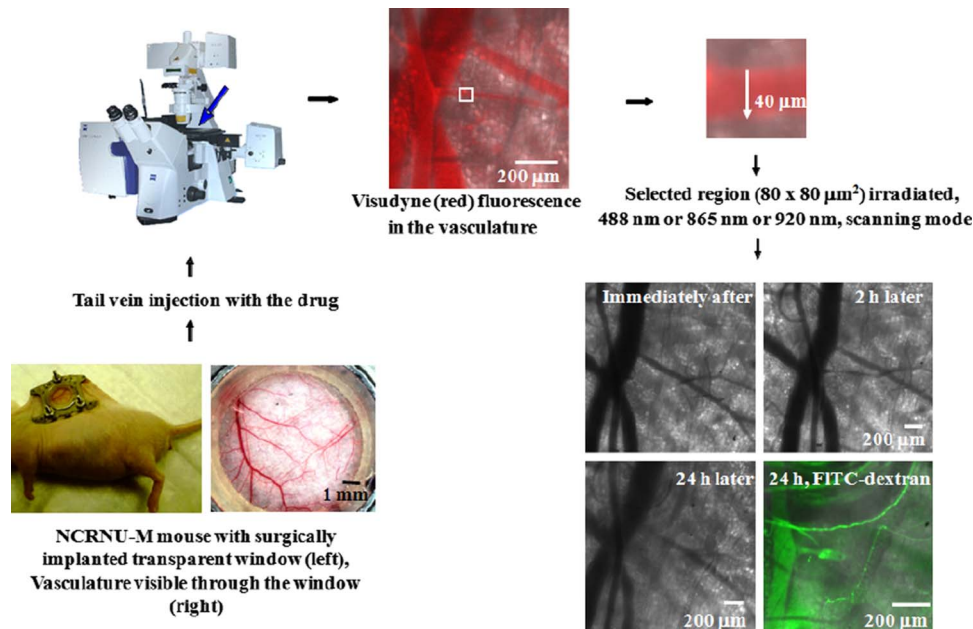
Fig. 1 Block diagram of the platform for localized PDT treatment *in vivo* and imaging of single blood vessels in the WCM model.

of central vision. While other treatments are now also being used for this condition,[16,17] it is likely that PDT will remain part of the therapeutic armamentarium, and clinical and preclinical studies combining PDT with anti-angiogenic treatments are in progress.[18,19] Currently, PDT for all approved indications uses single-photon excitation of the photosensitizer with a spatially distributed light treatment field—e.g., in the case of AMD, a red diode laser beam of a few mm diameter is targeted on the region of neovascularization. A potential limitation is that any photosensitizer that leaks into the retinal structures above or below the neovascular layer is also activated, leading to collateral damage that may contribute to the need for multiple repeat treatments.[20,21]

Over the past few years, we have been investigating two-photon (2-γ) activation,[22,23] in which nonlinear light absorption confines the PDT damage to a (diffraction limited) 3-D focal spot.[24,25] This can be achieved by scanning a tightly focused femtosecond (fs) laser beam across a defined volume of the neovascularization or by targeting the feeder vessels[26] that supply the neovascular zone. Recently, colleagues at University of Oxford have designed and synthesized porphyrin dimer-based photosensitizers with very high 2-γ cross section: up to $\sim 17{,}000$ GM units [1 GM $= 10^{-50}$ cm^4 s], which is orders of magnitude higher than conventional single-photon PDT compounds. We have reported successful 2-γ PDT shutdown of single targeted blood vessels using one such compound.[27] For this, we used the well-established WCM model,[28] described in the following, that allows one to visualize and target individual vessels in a minimally-invasive way. In the present work, we have used this model to investigate whether or not there is reciprocity of the single-vessel response to varying photosensitizer and light doses, as has been demonstrated for conventional wide-field PDT.[29,30] This

is important to guide the further development of single-vessel targeted treatments. Due to the limited supply of the porphyrin dimer compounds currently available, we have used verteporfin for these experiments to validate the principle of drug-light reciprocity for single-vessel focal PDT. We then compare the drug-light product required for vessel closure between 1-γ and 2-γ activation, between focal and broad-beam irradiation, and between verteporfin and the porphyrin dimer. This allows us to bridge these different approaches and to reach quantitative conclusions on the efficacy and clinical practicality of focal PDT for AMD and other microvascular pathologies. Moreover, since the subsequent photochemistry is the same for 1-γ and 2-γ excitation,[31] namely, singlet oxygen formation, the biological responses observed from the focal 1-γ study should be directly transferable to 2-γ excitation.

2 Methods

All animal studies were done with institutional approval (Protocol 1498, University Health Network, Toronto, Canada). The WCM model has been described in detail elsewhere:[28] briefly, a transparent window (1 cm in diameter) was surgically placed into the dorsal skin of nude mice (NCRNU-M, ~ 25 g) under general anesthesia (induced by intraperitoneal 80 mg kg^{-1} Ketamine plus 10 mg kg^{-1} Xylazine, with subsequent lower doses as required). As seen in Fig. 1, this allows direct visualization of the skin vasculature at high resolution under confocal microscopy.

Imaging and PDT treatments were performed using a confocal laser scanning microscope (LSM 510 Meta NLO; Carl Zeiss, Germany), coupled to either a continuous wave (CW) argon-ion laser (488 nm) or a Ti:sapphire laser (Chameleon; Coherent) that was tunable from 720 to 960 nm with 300-fs

pulse duration and 90-MHz repetition rate. Both transmission and fluorescence images were recorded. Imaging of the verteporfin fluorescence in the vasculature (argon-ion laser, subtherapeutic 10-μW power, $\lambda_{ex}=488$ nm, $\lambda_{em}=650$ to 710 nm) and the transmission images were used to guide selection of the blood vessel to be treated. Digital real-time imaging of the treated region was performed before, during and after the PDT treatment. Stereomicroscopy (MZ FLIII, Leica; $\times 1-8$ magnification, white-light mode) was used to image the whole vasculature in the dorsal window before and after PDT. These images allowed the treated region to be relocated at the different time points.

For the PDT treatments, carried out at $\geqslant 2$ h following implantation of the window, the photosensitizer was administered by bolus tail-vein injection in 5% dextrose: either verteporfin (molecular weight 718.8, 2 to 32 mg kg^{-1} body wt $\equiv 2.8$ to 44.5 micromoles kg^{-1}) or the porphyrin dimer[27] (molecular weight 2232.7, 10 mg kg^{-1} $\equiv 4.5$ micromoles kg^{-1}). The window chamber was then positioned under the microscope, and a suitable vessel was selected: for these studies, arteries (identified by wall thickness and direction of blood flow) of 40 to 50 μm lumenal diameter were used. A small region (80×80 μm^2) centered on the selected blood vessel was then irradiated in raster-scanning mode. The CW argon laser was used for verteporfin 1-γ focal PDT ($\lambda_{ex}=488$ nm, $5 \times$ dry objective, NA 0.25, 177-μW power at the tissue, 2700 mW cm^{-2} incident intensity, 1.60-μs pixel dwell time, spot size ~ 1.2 μm). For 2-γ PDT, the pulsed Ti:sapphire laser was used ($\lambda_{ex}=865$ nm for verteporfin, 920 nm for the porphyrin dimer, ~ 40 mW average power, irradiation done as a vertical stack of five images, each 10 μm apart, pulse length 300 fs at the sample position, $\sim 3.2 \times 10^{10}$ W cm^{-2} peak power intensity, 1.60-μs pixel dwell time, ~ 500-nm spot size). Light irradiation was started 15 min after photosensitizer injection, when the drug is primarily still in the vasculature. For the verteporfin dose-response experiments, the incident irradiance was varied in the range 40 to 3000 J cm^{-2} by increasing the treatment time in the range 38 s to 47 min. The treated region was imaged immediately after treatment and at 2 to 3 h and 17 to 25 h post-PDT treatment. For the latter, 5 mg kg^{-1} of 464,000 MW dextran labeled with fluorescein isothiocyanate (FITC; Sigma-Aldrich, Ontario, Canada) in 200 μl saline was injected i.v., and its fluorescence was imaged 15 min later ($\lambda_{ex}=488$ nm, $\lambda_{em}=500$ to 550 nm, 5-μW power). Mice were kept normothermic on a heated stage (30°C) during imaging and treatment.

Following imaging at the last time point, the mouse was euthanized by cervical dislocation. Surgically exposed dermis within the window was resected and fixed in 10% buffered-formalin for >48 h. The tissue was then paraffin embedded, sectioned (6 μm thickness) parallel to the skin surface and stained with haematoxylin and eosin (H&E). The sections were then imaged with a bright-field whole-slide scanner (ScanScope XT: Aperio, San Diego, California).

Where necessary to extend the previous literature and our own earlier work, a series of complementary studies was done to allow comparison of the drug-light product (DLP) for vascular occlusion using these 1-γ focal verteporfin-mediated PDT responses with other treatment conditions, including 2-γ treatment, wide-field irradiation, and/or the use of the porphyrin dimer. We will also compare these *in vivo* dose responses with those for corresponding *in vitro* cell effects, as reported previously.[32] Briefly, for the latter, a monolayer of endothelial cells was incubated with 10 μM verteporfin in the dark for 3 h. Next, a 230×230 μm^2 region of cells was selected and irradiated with 865-nm laser light. Cell viability stains were added 4 h later to obtain two-color visualization of live and dead cells.

For the broad-beam PDT experiments, a collimated beam from a 690-nm laser coupled to optical coherence tomography (OCT) system was delivered over a ~ 1.5-mm-diam spot. Blood flow in the targeted and surrounding region was recorded pre- during, and post-PDT using speckle variance OCT (sv-OCT).[33] For the PDT treatment, a total light dose 100 J cm^{-2} was delivered over 10 min at an incident power density of 166 mW cm^{-2}. In order to prevent any additional PDT damage, lower power from a 1300-nm laser was used in the sv-OCT instrument to record pre and post-PDT images. The sv-OCT method utilizes a speckle variance detection technique that is based on detection of changes in the successive structural images, as reported in detail previously.[33]

3 Results

An illustration of the setup and the scheme for the vascular response experiments is presented in Fig. 1, which shows the vasculature visible through the window using the stereomicroscope and the small treatment area of the targeted vessel using confocal microscopy. Figure 2 shows examples pre- and post- (0 h, 2 to 3 h, 17 to 25 h) PDT, illustrating the vascular response of arterioles (40 to 50 μm diameter) to different doses of verteporfin and focal 1-γ light activation. Changes in the targeted artery (shutdown, tapering, and FITC-dextran leakage or obstruction) were recorded at each time point following treatment. Figure 2(a) shows the localized vascular PDT response ($\lambda_{ex}=488$ nm) for 2.8 micromoles kg^{-1} verteporfin at a fluence of ~ 2700 J cm^{-2}. In this case, although immediate (0 h) occlusion was observed, the follow-up images (2.5 h and 22 h) showed arteriole rebound, confirmed by fluorescein-dextran dye permeation through the targeted region. With 5.6 micromoles kg^{-1} and ~ 1670 J cm^{-2} vasodilation of the targeted arteriole was seen [Fig. 2(b)]. There was also apparent damage to a nearby venule, outside the direct laser-beam treatment zone. While complete occlusion was not seen at 11.1 micromoles kg^{-1} and ~ 600 J cm^{-2} [Fig. 2(c)], the 24 h response showed swelling and hyperfluorescence of fluorescein in the treated area. Figures 2(d) and 2(e) show vessel responses for 22.3 and 44.5 micromoles kg^{-1} drug with light doses of ~ 400 and 325 J cm^{-2}, respectively. Both demonstrated permanent damage to the targeted arteriole, confirmed by FITC-dextran dye absence/obstruction in the treated region. No such response was observed in the light-only control [Fig. 2(f)], even though a high light dose (1340 J cm^{-2}) was deposited.

Figure 3 show scatter plots of the light doses corresponding to different degrees of vascular response at different time
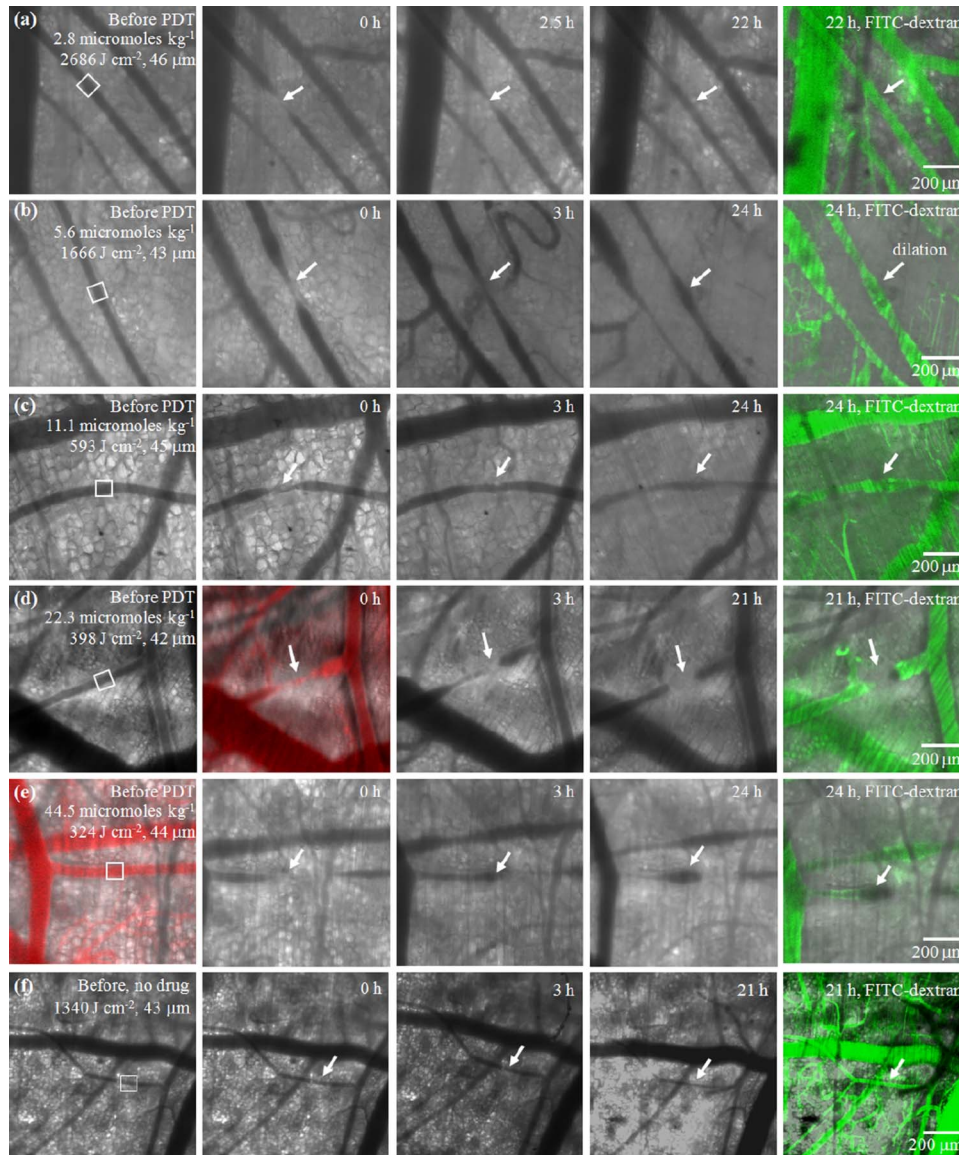
Fig. 2 Confocal microscope example images of different drug (2.8 to 44.5 micromoles kg^{-1} and no drug control) and light doses (320 to 2700 J cm^{-2}, $\lambda_{ex}=488$ nm, $5\times$ dry objective, NA 0.25, 177-μW power at the sample position, 2700 mW cm^{-2} incident intensity, 1.60-μs pixel dwell time, spot size ~1.2 μm) pre- and post-PDT (immediately after: 0 h; short-term: 2 to 3 h; long-term: 21 to 25 h). A few examples of verteporfin (red) fluorescence are also shown. Green fluorescence is due to FITC-labeled dextran injected at the longer time point. The treated arteriole (80×80 μm^2) region is marked with a white square and indicated by arrows. (Color online only.)

points post-PDT. Each symbol represents one mouse or vessel, which was tracked to assess the changes over time following treatment. These plots were generated as follows: for a given drug dose, the light dose was varied using 1 (or in some cases, 2) animals per dose until the targeted artery demonstrated leakage or occlusion, confirmed by fluorescein-labeled dextran dye injection at the 17 to 25 h time point. Once the approximate light dose to produce this response was known, the light dose was varied on either side of this value in several animals ($n \geqslant 3$) to determine the light dose required for occlusion of the arteriole at that particular drug dose. This was then repeated for a different drug doses. The sequence of drug

doses and the light dose ranging was random to minimize systematic bias. A single arteriole was targeted in most animals, except in a few cases at the higher drug doses for which the PDT treatment time was short (<200 s) and two well-separated and unconnected vessels could be used. Each point in the scatter plots has been color-coded according to whether the specific vessel response was (red) or was not (green) observed. Since these responses were clear and unequivocal, we relied on a single trained observer (MK), who was blinded to the light dose.

Independent of the drug dose, it was observed that the immediate vessel closure (shutdown at 0 h) does not necessarily predict the 17 to 25 h response, and that the irradiated
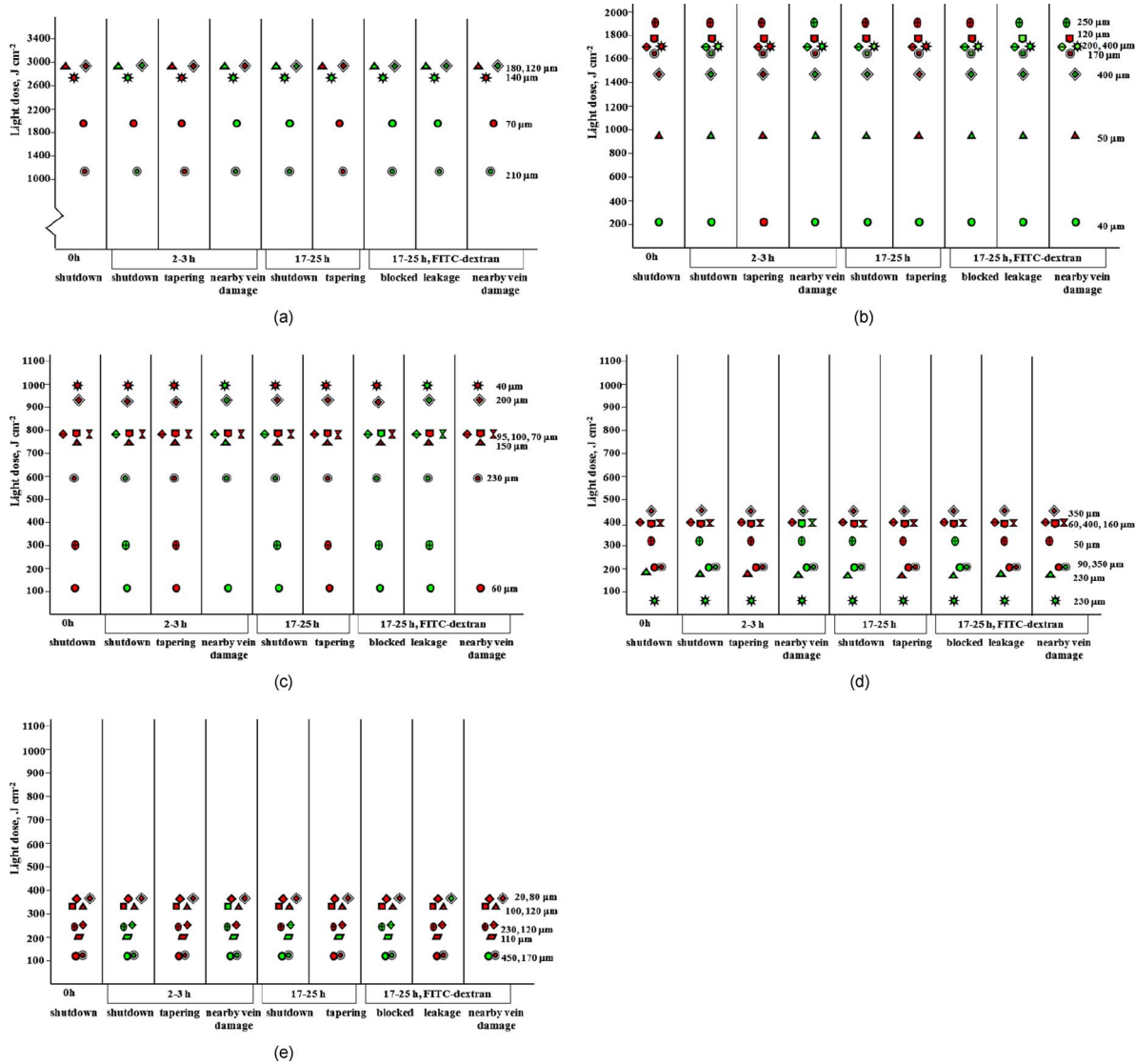
Fig. 3 Scatter diagram of single arteriole response to verteporfin focal 1-γ PDT in the WCM: (a) 2.8 micromoles kg^{-1}, 40 to 48 μm; (b) 5.6 micromoles kg^{-1}, 40 to 52 μm; (c) 11.1 micromoles kg^{-1}, 40 to 48 μm; (d) 22.3 micromoles kg^{-1}, 40 to 48 μm; (e) 44.5 micromoles kg^{-1}, 42 to 55 μm. A small region (80$\times$80 μm^2) of an artery was irradiated using an argon-ion laser (λ_{ex}=488 nm, incident intensity 2700 mW cm^{-2}, pixel dwell time 1.60 μs) 15 min after intravenous drug injection. Each row (with one type of symbol) represents one mouse, which is followed for various vascular responses at different time points. The *x* axis shows different time points and parameters that were observed, and light fluence values are shown on the *y* axis. Red color symbols indicate positive score, i.e., vascular shutdown, tapering, nearby vein damage, and dye blockage and/or leakage, and green implies negative score. Numbers on the extreme right side indicate the distance of the nearest vein to the targeted artery. (Color online only.)

arteriole can "rebound" if the PDT drug/light dose is not adequate. However, the short-term (2 to 3 h) responses are a good indicator of the long-term responses, as shown in Fig. 3(c) for 11.1 micromoles kg^{-1}: here, lower light fluences ($<$700 J cm^{-2}) resulted in immediate vessel closure but rebounded at the 2 to 3 h time point, whereas larger light doses ($>$700 J cm^{-2}) produced both short- and long-term closure, with FITC-dextran blockage and/or leakage.

As indicated earlier, we also observed narrowing of venules that were close to the targeted arterioles, but outside the light treatment field. Damage to the adjacent vein de-

pended on number of factors: the drug and light doses, the distance between the targeted artery and the vein, and the size of the vein. In the case of the lowest dose of 2.8 micromoles kg^{-1}, the effect was noticeable above 2000 J cm^{-2} for distances of 70 to 180 μm. At 5.6 micromoles kg^{-1}, damage to the nearest vein (50 to 170 μm) was seen above 900 J cm^{-2}, but there was no damage apparent beyond 200 μm, even at high light dose ($\geqslant$1500 J cm^{-2}). In the case of 11.1 to 44.5 micromoles kg^{-1}, damage was noticed in nearly all experiments with light doses as low as 200 J cm^{-2}. This damage to nearby veins could be due to scattered light,
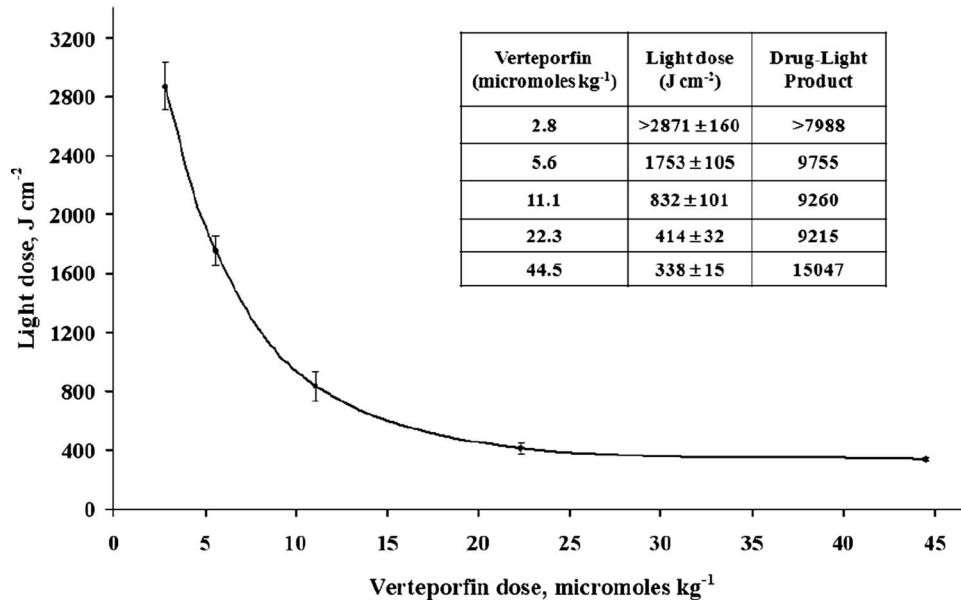
Fig. 4 Drug and light dose-response curve for single vessel occlusion in the WCM. Fluence values for localized vessel occlusion were obtained from the scatter diagram shown in Fig. 3. The x and y axis show escalating verteporfin (2.8 to 44.5 micromoles kg^{-1}) and light doses (J cm^{-2}). Error bars represent ± 1 s.d.

since the effect is not seen with 2-γ PDT.[27] In a small number of higher drug dose experiments [Figs. 3(d) and 3(e)] in which similar drug and light doses were delivered, we also noticed that this effect fell off with distance between the targeted artery and vein. Although there were only a few observation points, this suggests a secondary 'bystander' effect, possibly due to release of cytokines or other inflammatory elements in response to the damaged artery and surrounding tissue, which has previously been demonstrated in several PDT studies.[34,35]

The drug and light doses for vascular shutdown were then plotted against one another, as shown in Fig. 4. These values, together with corresponding DLP (Fig. 4, inset), were obtained from the scatter graphs of Fig. 3 by averaging the light doses for individual experiments that resulted in complete vessel shutdown at the 17 to 25 h time point for the respective drug doses ($n \geqslant 3$). For the 2.8 micromoles kg^{-1} data, we calculated the mean of the three highest light doses, since we could not achieve complete vessel occlusion. Hence, this DLP is the minimum value. It is seen that the light versus drug curve is well defined for focal irradiation and that, except for lowest and highest drug doses, the DLP is nearly constant. That is, the responses demonstrate photosensitizer-light reciprocity, consistent with a model in which the singlet oxygen generated is proportional to this product, implying that the treatments are not oxygen-limited. At the lowest drug dose of 2.8 micromoles kg^{-1}, a fluence of 2871 ± 160 J cm^{-2} was used for vessel shutdown, which necessitated a very long treatment time (~ 47 min), during which the concentration of circulating verteporfin likely dropped. Hence, one could expect breakdown of reciprocity in this case. At the highest drug dose of 44.5 micromoles kg^{-1}, the DLP also increased sig-

nificantly. This is most likely due to the vascular endothelial cells having reached a saturation concentration of photosensitizer, or it could be due to the very rapid narrowing of the lumen at this dose, which could limit the available oxygen during the irradiation.

Representative confocal microscopy and representative histopathology results are shown in Fig. 5, for both low- and high-dose PDT. With low-dose PDT [Fig. 5(a): 5.6 micromoles kg^{-1}, 1685 J cm^{-2}, DLP=9436], dilation of the targeted arteriole was noted by both confocal microscopy and subsequent histology of the same section. The latter demonstrated endothelial cell disruption in the treated area, indicated by an absence of nuclear staining along the inner vessel lumen. Despite apparent endothelial damage, the blood vessel was still patent, as demonstrated by the FITC-dextran dye permeation at 24 h after the PDT. However, for high-dose PDT [Fig. 5(b)], localized vessel occlusion was achieved (44.5 micromoles kg^{-1}, 340 J cm^{-2}, DLP=15130). Histology showed increased intra- and perivascular polymorphonuclear leukocytes in the treated vascular region, especially around the damaged endothelial lining. Cell death with signs of apoptosis (apoptotic bodies) as well as necrosis (karyorrhexis) was also visible. Histologic preparation of these thin tissue samples is challenging, especially to locate a very tiny region of a single blood vessel in a 1-cm-diam window, within which the entire vasculature is tortuous. Currently, we are refining the sectioning and staining methods to make this more reliable, but to date do not have good histology at other doses.

The drug-light products and the different experimental conditions for vascular occlusion under various drug and light regimes are summarized in Table 1, both for the WCM and for
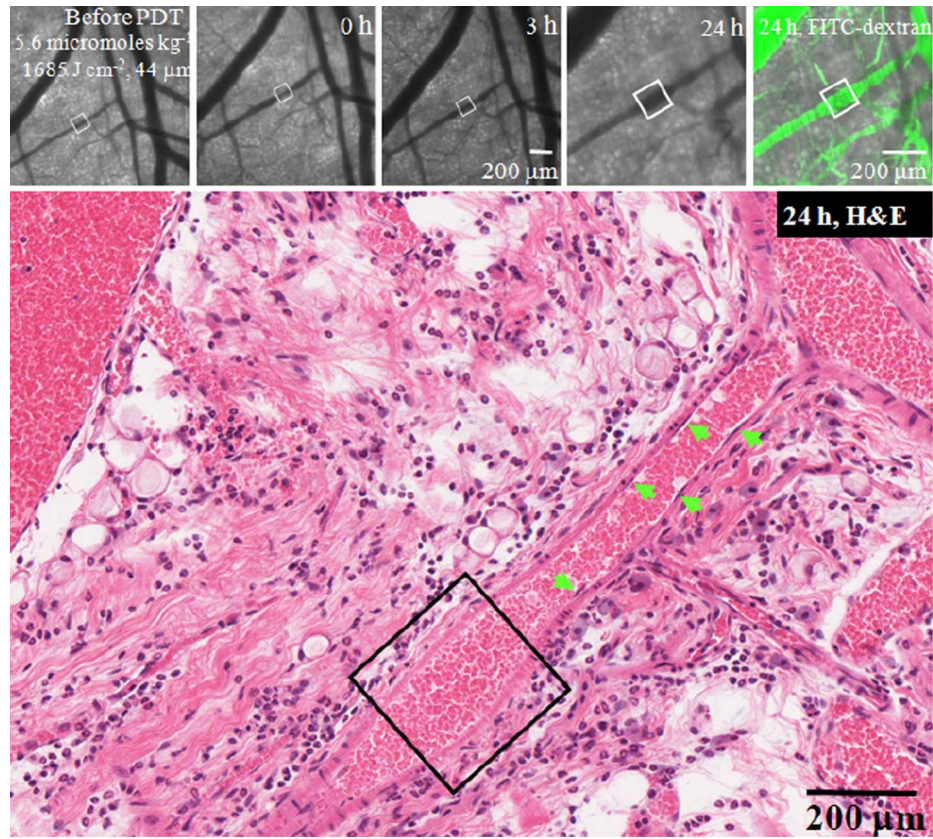
(a)
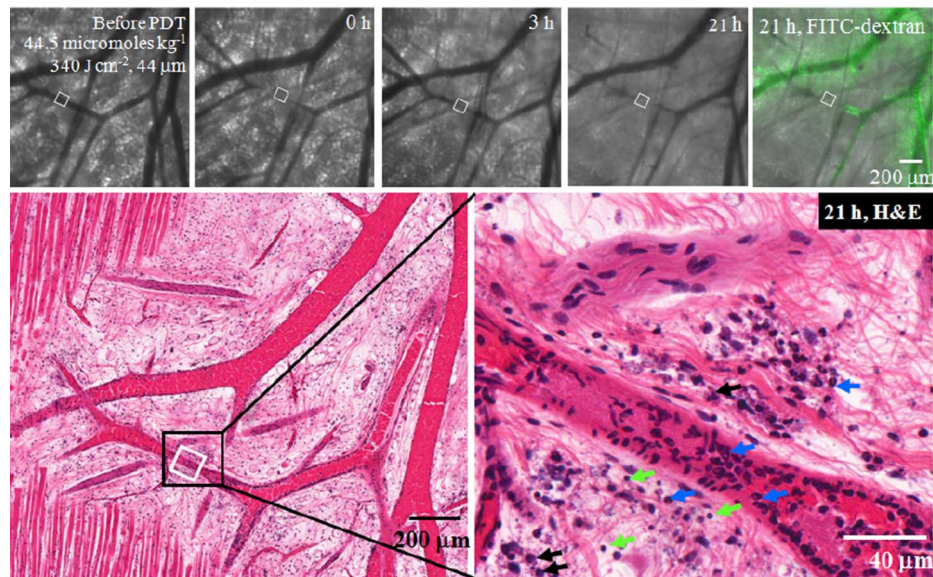
(b)

Fig. 5 Example confocal microscopy (top panel) before, immediately, and at 3 and 21 to 24 h post-verteporfin 1-γ PDT (λ_{ex}=488 nm, intensity 2700 mW cm^{-2}, pixel dwell time 1.60 μs) and histology for the same animal (lower panel) in the WCM. The targeted region (80 μm $\times$ 80 μm) is indicated by a white square or arrows. The image on the right shows a zoomed picture of the targeted region. (a) 5.6 micromoles kg^{-1}, 1685 J cm^{-2}. Dilation of the targeted arteriole can be seen at later time points in both transmission and fluorescence (FITC-dextran, green) images. Histology shows damage to endothelial cells, indicated by the absence of darkly stained nuclei in the treated region, which are indicated with green arrows for the intact endothelial lining in the nearby region. (b) 44.5 micromoles kg^{-1}, 340 J cm^{-2}. Occlusion of the targeted arteriole can be seen at later time points in both transmisison and fluorescence (FITC-dextran, green) images. Histology shows intra- and perivascular accumulation of poly-morphonuclear cells (blue arrows) in the treated region. Cells with signs of apoptosis (apoptotic bodies, green arrows), as well as necrosis (karyorrhexis, black arrows), are also visible in the surrounding region. (Color online only.)

Table 1 Summary of verteporfin 1- and 2-γ PDT and dimer 2-γ PDT for ~40-μm arteriole occlusion in dorsal window mice. Also shown are results for 50-μm arteriole conclusion in the CAM model.

| | Dorsal skinfold window chamber model, 40 μm | | | | CAM, 50 μm (Ref. 36) |
| | Verteporfin | | Dimer (Ref. 27) | | Verteporfin |
	1-γ	1-γ broad beam		2-γ	
Photomsensitizer conc. (micromoles kg^{-1})^a	22.3	1.4	44.5	4.5	2.8
Wavelength (nm)	488	690	865	920	780
Pulse width (femtosecond)	—	—	300	300	100
Magnification and numerical aperture of treatment spot	5×, 0.25	—	5×, 0.25	5×, 0.25	20×, 0.4
Peak irradiance (W cm^{-2})	2.7	0.17	3.2×10^{10}	3.2×10^{10}	3.7×10^{11}
J cm^{-2}	414	100	6.5×10^5	3.2×10^5	1.1×10^8
Treatment time (min)^b	6.5	10	24	12	5
Drug-light product (conc., micromoles kg^{-1} and fluence, J cm^{-2})	9215	140	2.9×10^7	1.4×10^6	3.1×10^8

^{a}Photosensitizer concentrations were converted to micromoles kg^{-1} by taking into account their molecular weights.
^{b}Includes the laser sleep time during focal 1- and 2-γ scanning irradiation PDT.

the chorioallantoic membrane (CAM) model in chick eggs,[36] which we have also used to assess the 2-γ PDT vascular response. Both 1-γ focal and broad-bream irradiation with verteporfin are compared, as well as 2-γ PDT with both verteporfin and the Oxford porphyrin dimer.[27] There are several points to note.

1. The DLP for focal irradiation is ~1.5 orders of magnitude higher than that for broad-beam irradiation.

2. With verteporfin the DLP is >3 orders of magnitude higher for 2-γ than for 1-γ activation, but this partially compensated by the much higher 2-γ cross section with the porphyrin dimer.

3. For 2-γ activation with verteporfin, the DLP for CAM vessels is an order of magnitude higher than for vessels in the WCM.

The first point clearly raises questions about the biology of the single vessel responses, which will be discussed in the following. The second point relates primarily to the low probability of 2-γ absorption in conventional photosensitizers and the need for "designer" drugs for this application. We note, however, that the full potential of the 300-fold higher 2-γ cross section in the dimer compared with verteporfin is not realized, most likely due to its poorer pharmacokinetics and/or microdistribution. With regard to the third point, an order of magnitude lower DLP in window chamber vessels could be due to slightly different vessel sizes (40 to 50 μm in the WCM versus 50 μm in the CAM model) or, more likely, to differences in the way light or drug is delivered. For the CAM studies, treatment was delivered to a single fixed spot (37 μm^3) on

the vessel wall, whereas in the WCM the laser beam was scanned over a larger area (80 μm × 80 μm) and through different layers (z sections: series of five depths 10 μm apart) of the blood vessel. This intermittent treatment may allow for oxygen and/or circulating photosensitizer replenishment. In the WCM, the photosensitizer was administered by tail-vein injection, remote from the target vessel, whereas in the CAM model injection was directly into the target vessel, just upstream of the irradiated spot. Also, the wavelength and 2-γ

Table 2 Scoring scale for assessing vascular occlusion in the CAM model.

Vascular occlusion rating (VOR)	Amount of vessel closure (AVC)
0	No visible change (AVC=0%)
1	Slight decrease (0%<AVC<50%)
2	Vessel diameter decrease by half (AVC=50%)
3	Lerge decrease (50%<AVC<100%)
4	Fully closed (AVC=100%)

Table 3 Summary of vascular occlusion ratings (VORs) in the CAM model with 2.8 micromoles kg^{-1} verteporfin 2-γ PDT.

Vessel diameter (μm)	VOR
20	4
30	4
50	4
80	3.25

cross-section values for verteporfin were different: 780 nm ($\sigma_2 \sim 60$ GM units) for the CAM experiments and 865 nm ($\sigma_2 \sim 30$ GM) in the case of the WCM,[37] which should make CAM vasculature even more responsive. Whatever the reason, it is surprising that the normal vessels in the WCM model appear to be more sensitive than the neovasculature in the CAM model, since other studies have suggested that neovasculature is more susceptible to PDT damage than normal vessels.[7,38,39]

There has been previous work on optimizing 2-γ PDT in the CAM model.[36] Vascular shutdown was attempted for a range of vessel diameters (20, 30, 50, 80 μm), occlusion being achieved for all except the largest, and the effect of laser power (30, 38, 45 mW) was also investigated for occlusion of 50-μm-diam arteries. For all these experiments, a verteporfin dose of 2.8 micromoles kg^{-1} was used, and 2-γ activation was carried out at 780 nm. Vascular constriction/occlusion was observed immediately after PDT. The results are summarized in Tables 2–5 and Fig. 6. The largest blood vessels tested (80 μm) showed significant vasoconstriction immediately after treatment, but complete vessel occlusion was not observed. It is possible that, if these vessels were imaged at longer times

Table 5 Vascular occlusion ratings for the optimized treatment of 50 μm vessels in the CAM model. For these experiments, verteporfin was injected into a feeder artery, upstream of a vessel branch and in the direction of the blood flow. 10 min after the start of infusion, 2-γ excitation PDT treatment was delivered using 780 nm pulsed laser light focused onto the upper portion of the lumen.

		Laser power (mW)		
		30	38	45
Treatment time (s)	60	0.2	0.8	2.2
	180	2.2	3.4	4
	300	3.4	4	4

after treatment, then complete vessel occlusion would be observed. The light dose was further optimized by treating 50-μm-diam arteries and showed that vessels could be occluded with a variety of high laser powers and long treatment times. It was determined that treatment with 45 mW could cause long-term vessel closure with as little as 3 min exposure, while longer irradiation times (5 min) were required to occlude vessels at a lower power (38 mW). It is likely then that, if either the drug or light dose were increased, occlusion of larger vessels would also be observed immediately after treatment. Additionally, using a photosensitizer with a high 2-γ cross section would also likely increase the vessel diameter that could be treated under such conditions.

4 Discussion

Earlier dose-dependence studies with different photosensitizers in various tumor and vascular models have used broad-beam light to target large (mm–cm) tissue areas that include numerous arteries and veins, and demonstrated that

Table 4 Light treatment parameters for optimization of 2-γ PDT of 50-μm arteries in the CAM model.

| Treatment time (s)	Light dose parameters	Laser power at the artery (mW)		
		30	38	45
60	Average irradiance (W cm^{-2})	2.54×10^6	3.18×10^6	3.81×10^6
	Peak irradiance (W cm^{-2})	2.91×10^{11}	3.64×10^{11}	4.37×10^{11}
	Fluence (J cm^{-2})	1.77×10^7	2.21×10^7	2.65×10^7
180	Average irradiance (W cm^{-2})	2.54×10^7	3.18×10^6	3.81×10^6
	Peak irradiance (W cm^{-2})	2.91×10^{11}	3.64×10^{11}	4.37×10^{11}
	Fluence (J cm^{-2})	5.31×10^7	6.63×10^7	7.96×10^7
300	Average irradiance (W cm^{-2})	2.54×10^6	3.18×10^6	3.81×10^6
	Peak irradiance (W cm^{-2})	2.91×10^{11}	3.64×10^{111}	4.37×10^{11}
	Fluence (J cm^{-2})	8.84×10^7	1.11×10^8	1.33×10^8
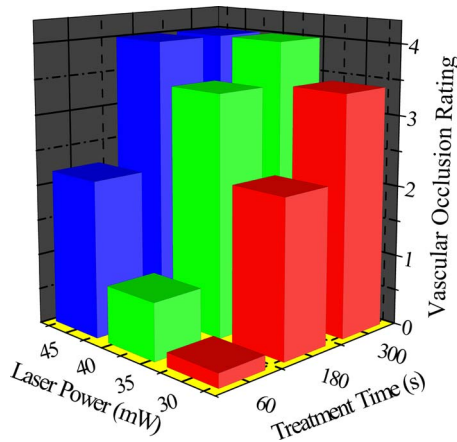
Fig. 6 Optimization of 2-γ PDT light dose in the CAM model. Each vessel was assigned a VOR based on the decrease in vascular size (Table 3) and plotted against the total length of time over which the light was delivered, and the delivered power at the vessel. Each point represents the average VOR for 5 vessels in 5 different eggs, and is a visual representation of Table 5.

Fig. 7 Example image of verteporfin (1.4 micromoles kg^{-1}) broad-beam PDT (690 nm, spot size ~1.5 mm in diameter in the center of the image, 100 J cm^{-2} fluence delivered over 10 min) in the WCM. The orange-red (false color) is the blood flow map using speckle variance OCT.[33] The 24 h time point vascular response image shows vascular shutdown of numerous vessels, ~50 μm vessels. (Color online only.)

photosensitizer-light dose reciprocity holds provided that oxygen is readily available. For example, Fingar et al.[29] showed drug-light reciprocity in intradermally implanted RIF tumors using the end-point of *ex vivo* tumor cell clonogenicity over a range of drug (dihematoporphyrin ether, 3 to 10 mg kg^{-1}) and light (40 to 135 J cm^{-2}) doses. In a follow-up study,[30] they demonstrated breakdown of reciprocity when the photosensitizer dose was reduced further and attributed this to photobleaching of the photosensitizer. Several other investigators have also evaluated the drug and light dose dependence of PDT effects *in vitro* using various porphyrin-based photosensitizers.[40,41]

The confirmation of drug-light dose reciprocity in focal PDT of individual blood vessels provides a high level of confidence that the model and evaluation metrics used in these experiments provide a robust platform for quantitative evaluation of this novel PDT approach. This is a necessary step toward applying the method to, for example, ocular models of AMD, which have significant additional technical challenges, particularly in achieving diffraction-limited focal irradiation given the limited numerical aperture of the eye and unavoidable optical aberrations.

The vessel responses in the present study were assessed by a single observer, which may be a weakness. However, the individual was blinded to the light dose used, and the responses are rather clear and unequivocal, so that we do not believe that this introduced undue bias: once vessel closure had been observed at a particular drug dose, multiple animals were treated with the light dose varied around this representative value to give a degree of statistical reliability.

With regard to the specific vascular responses, during irradiation we noticed immediate vasoconstriction for high verteporfin doses (22.3 and 44.5 micromoles kg^{-1}), whereas for low drug doses, slight transient dilation of the targeted arteriole was noticed first, followed by constriction. Subsequently, either recovery, tapering, and/or shutdown occurred, depending on the drug and light doses. Over two decades ago, Star et al., using a rat window chamber model, observed immediate
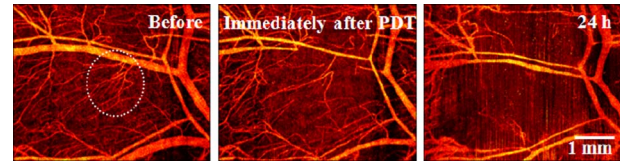
constriction and vasodilatation of tumor vasculature preceding complete stasis, when a large tissue area comprising multiple vessels was treated with hematoporphyrin derivative-mediated PDT.[42] In a 1989 publication,[43] Reed et al. compared the effects of (dihematoporphyrin ether) PDT on normal and tumor blood vessels and reported that vasoconstriction was predominant in arterioles, while venules showed mainly a thrombotic response. Fingar et al. performed a number of broad-beam PDT studies using several tumor models and investigated in detail the role and mechanisms of tumor microvascular damage.[7,44–47] In the present study, we did not examine the mechanism of localized vascular damage in detail. However, the current observations and these earlier large-area vascular PDT reports indicate that the underlying phenomena are similar, regardless of whether they are initiated by localized or broad-beam irradiation.

In the present study we detected disruption of the endothelial cell layer in the treated region (indicated by the absence of darkly stained flat nuclei along the inner vessel wall lining: Fig. 5), which has previously been established as the initial event before platelet aggregation at the damaged site.[7,8] This then leads to increased vascular permeability and eventually vessel shutdown, depending on the drug and light dose. In the case of high-dose focal PDT, we noticed polymorphonuclear leukocytes along the vessel lining (and in the surrounding area) that are normally limited to the blood circulation. Endothelial cell damage, followed by platelet aggregation and increase in vascular permeability leading to leakage of leukocytes in the treated area, have been reported previously in broad-beam PDT studies.[48–51] Also, cells undergoing both apoptosis and necrosis were observed around the targeted vascular region [Fig. 5(b)], which has likewise been reported.[52,53] These observations further point out to the fact that the mechanistic basis for localized and area vascularly targeted PDT is similar.

4.1 Comparisons with Other Treatment Conditions

Having determined the threshold DLP for single microvessel occlusion using focal 1-γ verteporfin PDT *in vivo*, it is of interest to compare this with other treatment conditions. First, as shown in the example in Fig. 7, for broad-beam 1-γ PDT (spot size 1.5 mm), only a very low DLP (1.4 micromoles kg^{-1} × 100 J cm^{-2}) was required for permanent vessel closure of a region containing numerous arteries and veins (40 to 50 μm diameter). The damage boundary was nearly twice the diameter of the treated area, which could
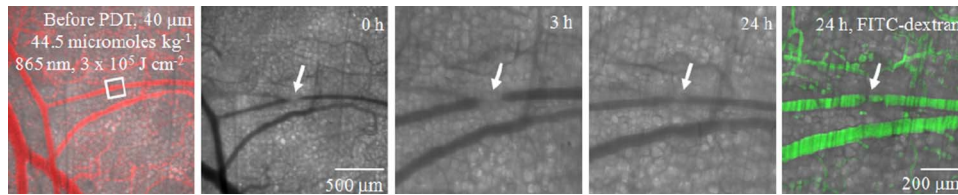
Fig. 8 Example of verteporfin (44.5 micromoles kg^{-1}) 2-γ PDT (865 nm, 5× dry objective, NA 0.25, ~3×10^5 J cm^{-2} fluence delivered over 12 min, ~40 mW average power, ~3.2×10^{10} W cm^{-2} peak power intensity, 1.60 μs pixel dwell time, spot size ~500 nm) in the WCM. Damage to the treated arteriole is noticeable both immediately and 3 h after PDT. The 24 h image shows some recovery, but tapering of the treated region is evident from the FITC-dextran fluorescence. Nearby veins did not show damage or inflammatory response, unlike in the case of focal 1-γ PDT (Fig. 2).

be a consequence of scattered light. By contrast, with focal treatment for 1-γ CW irradiation the local light fluence (~6000 J cm^{-2} for 1.4 micromoles kg^{-1} verteporfin, estimated from the dose-response curve shown in Fig. 4) required for vascular shutdown was 60 times higher than with broad-beam irradiation (100 J cm^{-2}). It is possible that there is localized oxygen depletion or ground-state photosensitizer depletion in the case of the focal treatment, since the fluence rate is 15 times higher (2700 versus 166 mW cm^{-2}). Such effects would reduce the effective PDT dose delivered. Alternatively, or in addition, the low DLP with wide-beam irradia-

tion could be due to the additive biological effect of the damage to multiple vessels (e.g., a cumulative bystander effect). It could also imply that it is much easier to close vessels if the PDT damage occurs along a substantial length of the vessel rather than at a single localized spot, and this is currently being investigated.

A second comparison is that between 2-γ PDT using verteporfin (Fig. 8) or the porphyrin dimer that we have reported previously.[27] With verteporfin, $DLP_{2-\gamma}$ was >3 orders of magnitude higher than $DLP_{1-\gamma}$. This is hardly surprising, since the 2-γ cross section of this photosensitizer is very low

Table 6 Summary of *in vitro* verteporfin 1- and 2-γ PDT using cell monolayers.

	1-γ focal	1-γ broad beam		2-γ	
	Khurana et al. (Ref. 32)	Nowak-Sliwinska et al. (Ref. 54)	Chen et al. (Ref. 55)	Khurana et al. (Ref. 32)	Karotki et al. (Ref. 22) (no drug, light only)
Photosensitizer conc. (micromoles kg^{-1})[a]	10.1	2.8	0.28	10.1	0
Wavelength (nm)	514	690	690	865	865
Pulse width (femtosecond)	—	—	—	300	300
Magnification and numerical aperture of treatment spot	40×, 1.2	—	—	40×, 1.2	40×, 1.2
Power (mW)	0.011	—	—	7.0	40
Drug incubation (min)	150	60	15	150	—
Park irradiance (W cm^{-2})	—	—	—	2.6×10^{11}	7.8×10^{11}
Confluent cell monolayer	YPEN-1 endothelial	S91 melanoma	SVEC4-10 endothelial	YPEN-1 endothelial	YPEN-1 endothelial
J cm^{-2}	0.14	0.04	1	1000	25000
Evaluation	90% killing	90% killing	Cell permeability loss	90% killing	bubble formation
Drug-light product (conc., micromoles kg^{-1}; fluence, J cm^{-2})	1.4	0.11	0.28	10^4	—

[a]Photosensitizer concentrations were converted to micromoles kg^{-1} by taking into account their molecular weights.

$(\sigma_2 \sim 50$ GM units).[32] However, unlike focal 1-γ PDT (Fig. 2), there were no visible signs of damage or inflammatory response to nearby veins. This suggests a possible alternative to the bystander interpretation—namely, that there is a significant contribution from scattered light even with the small focal spot and relatively thin tissue (~ 400 μm) in the WCM. The effects of such scattering would be much less in the case of the 2-γ irradiation, since the wavelength of the fs laser (865 nm) is beyond the 1-γ absorption range. When we switched to the porphyrin dimer that was designed *de novo* to have a very high 2-γ cross section ($\sigma_2 \sim 17,000$ GM units at 920 nm),[27] the DLP$_{2\text{-}\gamma}$ was 20-fold lower than for verteporfin. The fact that this reduction is much less than the 340-fold $(17,000/50)$ expected on the basis of the high 2-γ cross section relative to verteporfin suggests that the uptake and/or localization to PDT-sensitive sites are different, and this has been confirmed by *in vitro* fluorescence microscopy.[27] Further studies using targeted delivery vehicles for the dimer compound are in progress.

We also reviewed our previous *in vitro* results, summarized in Table 6, for endothelial cell kill using focal 1- and 2-γ verteporfin-PDT[32] and compared these with published verteporfin broad-beam *in vitro* experiments.[54,55] For similar cell kill, 1-γ focal PDT required 5 to 15 times higher DLP than broad-beam PDT: this is only a rough comparison, as the experiments were done under different conditions using different cell lines. The *in vitro* DLP$_{2\text{-}\gamma}$ was >3 orders of magnitude higher than for 1-γ focal PDT.

To our knowledge, there are no studies that have targeted a very small region with focal PDT in normal healthy blood vessels, but there have been several attempts to identify and occlude feeder vessels in patients. In a proof-of-principle study with 11 AMD patients (subfoveal occult CNV with feeder vessels <150 μm), Flower[56] demonstrated the feasibility of indocyanine green dye (ICG)–enhanced photocoagulation of these vessels with a device that permitted real-time visualization of the choroidal circulation while aiming the treatment laser beam. Feeder vessel closure could be achieved with 1 to 3 laser pulses, each of energy 0.6 J (7.6 $\times 10^3$ J cm^{-2}, ICG: 0.3 ml of 65 mg ml^{-1}; spot diameter: 100 μm; duration: 1.0 to 1.5 s; laser power 400 to 600 mW; 5096 to 7644 W cm^{-2}), with no visible damage to the surrounding fundus tissue. Staurenghi et al. mentioned the importance of ICG angiography in detecting small feeder vessels but also emphasized that the success of treating feeder vessels by (photothermal) laser depends on their width, length and number.[57] These reports indicate the necessity of a reliable real-time monitoring system for both identification of feeder vessels (or neovasculature) and evaluation of the therapeutic response. Research in this direction is already underway and one such emerging technique that we are exploring is sv-OCT.[58,59]

In summary, this is the first report of quantitative dose relationships for focal PDT targeting individual blood vessels *in vivo*, an approach that is greatly facilitated by the use of the WCM. Confirmation of photosensitizer–light dose reciprocity gives a basis for dose optimization, while the significant differences between focal and large-area vascular targeting raises significant questions about the biology of (micro)vascular responses to PDT-induced damage. We recognize that the current studies have been done in normal blood vessels, rather than in neovasculature such as found in AMD or tumors. Based on previous reports of the sensitivity of neovessels to PDT,[7,38] it is likely that the absolute values of the DLP for vascular occlusion are higher than will be required for treating such pathologic tissues. Conversely, this is not consistent with higher doses observed in the case of CAM vessel closure, despite local injection of the photosensitizer. However, we note that in the CAM experiments, the PDT dose was delivered at a spot close to the upper vessel wall, whereas in the WCM, a larger region was scanned circumferentially, encompassing more endothelial cells.

The ultimate goal of this study is to evaluate the efficacy of highly localized 2-γ PDT, either as stand-alone treatment or, most likely, in combination with other approaches for vascular pathologies where high spatial confinement is a significant potential advantage.

Acknowledgments

References

1. O. Raab, "On the effect of fluorescent substances on infusoria (in German)," *Z. Biol.* **39**, 524–546 (1900).
2. J. D. Spikes, "The historical development of ideas on applications of photosensitizer reactions to the health sciences," in *Primary Photoprocess in Biology and Medicine*, R. V. Bensasson, G. Jori, E. Land, and T. G. Truscott, Editors., pp. 209–227, Plenum Press, New York (1985).
3. R. L. Lipson and E. J. Baldes, "The photodynamic properties of a particular hematoporphyrin derivative," *Arch. Dermatol.* **82**, 508–516 (1960).
4. T. J. Dougherty, B. Henderson, S. Schwartz, J. W. Winkelman, and R. L. Lipson, "Historical perspective in photodynamic therapy," in *Photodynamic Therapy*, B. W. Henderson and T. J. Dougherty, Eds., pp. 1–18, Marcel Dekker, New York (1992).
5. T. J. Dougherty, J. E. Kaufman, A. Goldfarb, K. R. Weishaupt, D. Boyle, and A. Mittleman, "Photoradiation therapy for the treatment of malignant tumors," *Cancer Res.* **38**, 2628–2635 (1978).
6. M. A. Awan and S. A. Tarin, "Review of photodynamic therapy," *Surgeon* **4**, 231–236 (2006).
7. V. H. Fingar, "Vascular effects of photodynamic therapy," *J. Clin. Laser Med. Surg.* **14**, 323–328 (1996).
8. B. Krammer, "Vascular effects of photodynamic therapy," *Anticancer Res.* **21**, 4271–4277 (2001).
9. J. Trachtenberg, R. A. Weersink, S. R. H. Davidson, M. A. Haider, A. Bogaards, M. R. Gertner, A. Evans, A. Scherz, J. Savard, J. L. Chin, B. C. Wilson, and M. Elhilali, "Vascular-targeted photodynamic therapy (padoporfin, WST09) for recurrent prostate cancer after failure of external beam radiotherapy: a study of escalating light doses," *BJU Int.* **102**, 556–562 (2008).
10. B. Furie and B. C. Furie, "*In vivo* thrombus formation," *J. Thromb. Haemost.* **5**, 12–17 (2007).
11. L. Sikora, A. C. Johansson, S. P. Rao, G. K. Hughes, D. H. Broide, and P. Sriramarao, "A murine model to study leukocyte rolling and

intravascular trafficking in lung microvessels," *Am. J. Pathol.* **162**, 2019–2028 (2003).

12. S. Falati, P. Gross, G. Merrill-Skoloff, B. C. Furie, and B. Furie, "Real-time *in vivo* imaging of platelets, tissue factor, and fibrin during arterial thrombus formation in the mouse," *Nat. Med.* **8**, 1175–1181 (2002).

13. H. Sorg, J. N. Hoffmann, R. E. Rumbaut, M. D. Menger, N. Lindenblatt, and B. Vollmar, "Efficacy of antithrombin in the prevention of microvascular thrombosis during endotoxemia: an intravital microscopic study," *Thromb. Res.* **121**, 241–248 (2007).

14. M. Khurana, E. H. Moriyama, A. Mariampillai, and B. C. Wilson, "Intravital high resolution optical imaging of individual vessel response to photodynamic treatment," *J. Biomed. Opt.* **13**, 040502 (2008).

15. Verteporfin Roundtable 2000 and 2001 Participants, "Treatment of age-related macular degeneration with photodynamic therapy (TAP) study group principal investigators; Verteporfin in photodynamic therapy (VIP) study group principal investigators. Guidelines for using verteporfin (Visudyne) in photodynamic therapy to treat choroidal neovascularization due to age-related macular degeneration and other causes," *Retina* **22**, 6–18 (2002).

16. M. Waisbourd, A. Loewenstein, M. Goldstein, and I. Leibovitch, "Targeting vascular endothelial growth factor: a promising strategy for treating age-related macular degeneration," *Drugs Aging* **24**, 643–662 (2007).

17. V. Chaudhary, A. Mao, P. L. Hooper, and T. G. Sheidow, "Triamcinolone acetonide as adjunctive treatment to verteporfin in neovascular age-related macular degeneration: a prospective randomized trial," *Ophthalmology* **114**, 2183–2189 (2007).

18. J. Bradley, M. Ju, and G. S. Robinson, "Combination therapy for the treatment of ocular neovascularization," *Angiogenesis* **10**, 141–148 (2007).

19. M. Ju, C. Mailhos, J. Bradley, T. Dowie, M. Ganley, G. Cook, P. Calias, N. Lange, A. P. Adamis, D. T. Shima, and G. S. Robinson, "Simultaneous but not prior inhibition of VEGF165 enhances the efficacy of photodynamic therapy in multiple models of ocular neovascularization," *Invest. Ophthalmol. Vis. Sci.* **49**, 662–670 (2008).

20. D. N. Zacks, E. Ezra, Y. Terada, N. Michaud, E. Connolly, E. S. Gragoudas, and J. W. Miller, "Verteporfin photodynamic therapy in the rat model of choroidal neovascularization: angiographic and histologic characterization," *Invest. Opthalmol. Vis. Sci.* **43**, 2384–2391 (2002).

21. M. H. Reinke, C. Canakis, D. Husain, N. Michaud, T. J. Flotte, E. S. Gragoudas, and J. W. Miller, "Verteporfin photodynamic therapy retreatment of normal retina and choroid in the cynomolgus monkey," *Ophthalmology* **106**, 1915–1923 (1999).

22. A. Karotki, M. Khurana, J. R. Lepock, and B. C. Wilson, "Simultaneous two-photon excitation of Photofrin in relation to photodynamic therapy," *Photochem. Photobiol.* **82**, 443–452 (2006).

23. K. S. Samkoe and D. T. Cramb, "Application of an *ex ovo* chicken chorioallantoic membrane model for two-photon excitation photodynamic therapy of age-related macular degeneration," *J. Biomed. Opt.* **8**, 410–417 (2003).

24. R. M. Williams, D. W. Piston, and W. W. Webb, "Two-photon molecular excitation provides intrinsic 3-dimensional resolution for laser-based microscopy and microphotochemistry," *FASEB J.* **8**, 804–813 (1994).

25. M. Oheim, D. J. Michael, M. Geisbauer, D. Madsen, and R. H. Chow, "Principles of two-photon excitation fluorescence microscopy and other nonlinear imaging approaches," *Adv. Drug Delivery Rev.* **58**, 788–808 (2006).

26. I. Kozak, L. Cheng, D. E. Cochran, and W. R. Freeman, "Phase I clinical trial results of verteporfin enhanced feeder vessel therapy in subfoveal choroidal neovascularization in age related macular degeneration," *Br. J. Ophthalmol.* **90**, 1152–1156 (2006).

27. H. A. Collins, M. Khurana, E. H. Moriyama, A. Mariampillai, E. Dahlstedt, M. Balaz, M. K. Kuimova, M. Drobizhev, V. X. D. Yang, D. Phillips, A. Rebane, B. C. Wilson, and H. L. Anderson, "Blood vessel closure using photosensitizers engineered for two-photon excitation," *Nat. Photonics* **2**, 420–424 (2008).

28. G. H. Algire and F. Y. Legallais, "Recent developments in the transparent-chamber technique as adapted to the mouse," *J. Natl. Cancer Inst. (1940-1978)* **10**, 225–253 (1949).

29. V. H. Fingar, W. R. Potter, and B. W. Henderson, "Drug and light dose dependence of photodynamic therapy: a study of tumor cell clonogenicity and histologic changes," *Photochem. Photobiol.* **45**, 643–650 (1987).

30. V. H. Fingar and B. W. Henderson, "Drug and light dose dependence of photodynamic therapy: A study of tumor and normal tissue response," *Photochem. Photobiol.* **46**, 837–841 (1987).

31. R. L. Goyan and D. T. Cramb, "Near-infrared two-photon excitation of protoporphyrin IX: photodynamics and photoproduct generation," *Photochem. Photobiol.* **72**, 821–827 (2000).

32. M. Khurana, H. A. Collins, A. Karotki, H. L. Anderson, D. T. Cramb, and B. C. Wilson, "Quantitative *in vitro* demonstration of two-photon photodynamic therapy using Photofrin and Visudyne," *Photochem. Photobiol.* **83**, 1441–1448 (2007).

33. A. Mariampillai, B. A. Standish, E. H. Moriyama, M. Khurana, N. R. Munce, M. K. Leung, J. Jiang, A. Cable, B. C. Wilson, A. I. Vitkin, and V. X. Yang, "Speckle variance detection of microvasculature using swept-source optical coherence tomography," *Opt. Lett.* **33**, 1530–1532 (2008).

34. S. O. Gollnick, S. S. Evans, H. Baumann, B. Owczarczak, P. Maier, L. Vaughan, W. C. Wang, E. Unger, and B. W. Henderson, "Role of cytokines in photodynamic therapy-induced local and systemic inflammation," *Br. J. Cancer* **88**, 1772–1779 (2003).

35. B. W. Henderson, S. O. Gollnick, J. W. Snyder, T. M. Busch, P. C. Kousis, R. T. Cheney, and J. Morgan, "Choice of oxygen-conserving treatment regimen determines the inflammatory response and outcome of photodynamic therapy in tumors," *Cancer Res.* **64**, 2120–2126 (2004).

36. K. S. Samkoe, "Two-photon excitation photodynamic therapy: progress towards a new treatment for wet age-related macular degeneration," PhD Thesis, Department of Chemistry, University of Calgary (2007).

37. K. S. Samkoe, A. Clancy, A. Karotki, B. C. Wilson, and D. T. Cramb, "Complete blood vessel occlusion in the chick chorioallantoic membrane using two-photon excitation photodynamic therapy: implications for treatment of wet age-related macular degeneration," *J. Biomed. Opt.* **12**, 034025 (2007).

38. V. H. Fingar, S. W. Taber, P. S. Haydon, L. T. Harrison, S. J. Kempf, and T. J. Wieman, "Vascular damage after photodynamic therapy of solid tumors: a view and comparison of effect in preclinical and clinical models at the University of Louisville," *Rev. Gastroenterol. Peru* **14**, 93–100 (2000).

39. D. K. Kelleher, O. Thews, A. Scherz, Y. Salomon, and P. Vaupel, "Perfusion, oxygenation status and growth of experimental tumors upon photodynamic therapy with Pdbacteriopheophorbide," *Int. J. Oncol.* **24**, 1505–1511 (2004).

40. S. L. Gibson and R. Hilf, "Interdependence of fluence, drug dose and oxygen on hematoporphyrin derivative induced photosensitization of tumor mitochondria," *Photochem. Photobiol.* **42**, 367–373 (1985).

41. B. W. Henderson, D. A. Bellnier, B. Ziring, and T. J. Dougherty, "Aspects of the cellular uptake and retention of hematoporphyrin derivative and their correlation with the biological response to PRT *in vitro*," in *Porphyrin Photosensitization*, D. Kessel and T. J. Dougherty, Eds., pp. 129–138, New York, Plenum Press (1983).

42. W. M. Star, H. P. A. Marijnissen, A. E. van den Berg-Blok, J. A. C. Versteeg, K. A. P. Franken, and H. S. Reinhold, "Destruction of rat mammary tumor and normal tissue microcirculation by hematoporphyrin derivative photoradiation observed *in vivo* in sandwich observation chambers," *Cancer Res.* **46**, 2532–2540 (1986).

43. M. W. Reed, T. J. Wieman, D. A. Schuschke, M. T. Tseng, and F. N. Miller, "A comparison of the effects of photodynamic therapy on normal and tumor blood vessels in the rat microcirculation," *Radiat. Res.* **119**, 542–552 (1989).

44. V. H. Fingar, T. J. Wieman, S. A. Wiehle, and P. B. Cerrito, "The role of microvascular damage in photodynamic therapy: the effect of treatment on vessel constriction, permeability, and leukocyte adhesion," *Cancer Res.* **52**, 4914–4921 (1992).

45. V. H. Fingar, T. J. Wieman, and P. S. Haydon, "The effects of thrombocytopenia on vessel stasis and macromolecular leakage after photodynamic therapy using Photofrin," *Photochem. Photobiol.* **66**, 513–517 (1997).

46. V. H. Fingar, P. K. Kik, P. S. Haydon, P. B. Cerrito, M. Tseng, E. Abang, and T. J. Wieman, "Analysis of acute vascular damage after photodynamic therapy using benzoporphyrin derivative (BPD)," *Br. J. Cancer* **79**, 1702–1708 (1999).

47. V. H. Fingar, K. A. Siegel, T. J. Wieman, and K. W. Doak, "The

effects of thromboxane inhibitors on the microvascular and tumor response to photodynamic therapy," *Photochem. Photobiol.* **58**, 393–399 (1993).

48. M. O. Dereski, C. Hopp, Q. Chen, and F. W. Hetzel, "Normal brain tissue response to photodynamic therapy: histology, vascular permeability and specific gravity," *Photochem. Photobiol.* **50**, 653–657 (1989).

49. M. Korbelik, "PDT-associated host response and its role in the therapy outcome," *Lasers Surg. Med.* **38**, 500–508 (2006).

50. I. Cecic, C. S. Parkins, and M. Korbelik, "Induction of systemic neutrophil response in mice by photodynamic therapy of solid tumors," *Photochem. Photobiol.* **74**, 712–720 (2001).

51. J. Sun, I. Cecic, C. S. Parkins, and M. Korbelik, "Neutrophils as inflammatory and immune effectors in photodynamic therapy-treated mouse SCCVII tumours," *Photochem. Photobiol. Sci.* **1**, 690–695 (2002).

52. M. A. Middelkamp-Hup, I. Sánchez-Carpintero, S. Kossodo, P. Waterman, S. González, M. C. Mihm Jr., and R. R. Anderson, "Photodynamic therapy for cutaneous proliferative vascular tumors in a mouse model," *J. Invest. Dermatol.* **121**, 634–639 (2003).

53. J. W. Miller, "Higher irradiance and photodynamic therapy for age-related macular degeneration," *Trans.-Am. Acad. Opthalmol. Otolayngol., Sec. Ophthalmol.* **106**, 357–382 (2008).

54. P. Nowak-Sliwinska, A. Karocki, M. Elas, A. Pawlak, G. Stochel, and K. Urbanska, "Verteporfin, photofrin II, and merocyanine 540 as PDT photosensitizers against melanoma cells," *Biochem. Biophys. Res. Commun.* **349**, 549–555 (2006).

55. B. Chen, B. W. Pogue, J. M. Luna, R. L. Hardman, P. J. Hoopes, and T. Hasan, "Tumor vascular permeabilization by vascular-targeting photosensitization: effects, mechanism, and therapeutic implications," *Clin. Cancer Res.* **12**, 917–923 (2006).

56. R. W. Flower, "Optimizing treatment of choroidal neovascularization feeder vessels associated with age-related macular degeneration," *Am. J. Ophthalmol.* **134**, 228–239 (2002).

57. G. Staurenghi, N. Orzalesi, A. La Capria, and M. Aschero, "Laser treatment of feeder vessels in subfoveal choroidal neovascular membranes: a revisitation using dynamic indocyanine green angiography," *Ophthalmology* **105**, 2297–2305 (1998).

58. Y. Wang, A. Lu, J. Gil-Flamer, O. Tan, J. A. Izatt, and D. Huang, "Measurement of total blood flow in the normal human retina using Doppler Fourier-domain optical coherence tomography," *Br. J. Ophthamol.* **93**, 634–637 (2009).

59. M. E. J. van Velthoven, D. J. Faber, F. D. Verbraak, T. G. van Leeuwen, and M. D. de Smet, "Recent developments in optical coherence tomography for imaging the retina," *Prog. Retin Eye Res.* **26**, 57–77 (2007).